MOLECULAR AND CELLULAR BIOLOGY, May 1993, p. 2765–2775
0270-7306/93/052765-11$02.00/0

Vol. 13, No. 5

Zebra Fish *myc* Family and *max* Genes: Differential Expression and Oncogenic Activity throughout Vertebrate Evolution

NICOLE SCHREIBER-AGUS,[1] JIM HORNER,[1] RICHARD TORRES,[1] FUNG-CHOW CHIU,[2] AND RONALD A. DEPINHO[1]*

Department of Microbiology and Immunology[1] and Department of Neurology,[2] Albert Einstein College of Medicine, Bronx, New York 10461

Received 27 October 1992/Returned for modification 3 December 1992/Accepted 9 February 1993

To gain insight into the role of Myc family oncoproteins and their associated protein Max in vertebrate growth and development, we sought to identify homologs in the zebra fish (*Brachydanio rerio*). A combination of a polymerase chain reaction-based cloning strategy and low-stringency hybridization screening allowed for the isolation of zebra fish c-, N-, and L-*myc* and *max* genes; subsequent structural characterization showed a high degree of conservation in regions that encode motifs of known functional significance. On the functional level, zebra fish Max, like its mammalian counterpart, served to suppress the transformation activity of mouse c-Myc in rat embryo fibroblasts. In addition, the zebra fish c-*myc* gene proved capable of cooperating with an activated H-*ras* to effect the malignant transformation of mammalian cells, albeit with diminished potency compared with mouse c-*myc*. With respect to their roles in normal developing tissues, the differential temporal and spatial patterns of steady-state mRNA expression observed for each zebra fish *myc* family member suggest unique functions for L-*myc* in early embryogenesis, for N-*myc* in establishment and growth of early organ systems, and for c-*myc* in increasingly differentiated tissues. Furthermore, significant alterations in the steady-state expression of zebra fish *myc* family genes concomitant with relatively constant *max* expression support the emerging model of regulation of Myc function in cellular growth and differentiation.

The task of identifying genes governing key developmental decisions has been aided greatly by invertebrate systems such as *Caenorhabditis elegans* (24) and *Drosophila melanogaster* (37). Many of these pivotal genes appear to encode sequence-specific transcription factors (or their associated proteins) that serve to regulate the expression of target genes involved in normal growth and differentiation processes. Characterization of homologs of these invertebrate regulators in *Xenopus laevis*, the chicken, and the mouse has advanced our understanding of the mechanisms that control developmental processes in vertebrates. With the establishment of the zebra fish system by Streisinger et al. (45), many of the classical genetic approaches conducted exclusively in invertebrate model systems are now achievable in the framework of a vertebrate organism (25, 36). As a developmental genetic system, the zebra fish (*Brachydanio rerio*) appears ideal in that its embryos are highly accessible, the stages of early development are extremely rapid and well characterized, the generation time is relatively short, and the transparent nature and simple patterning of the zebra fish embryo readily permit a comprehensive phenotypic analysis. Moreover, external development allows for graft exchange studies and microinjection of DNA or RNA.

These experimental merits of the zebra fish, as well as its large phylogenetic distance from mammals, prompted our search for homologs of the Myc family and of its associated protein, Max, in the zebra fish genome. In higher vertebrates, the Myc family has been shown to consist of three highly related nuclear phosphoproteins, c-, N-, and L-Myc. Notable structural features of the Myc family include an amino-terminal domain with transactivation potential, a region rich in basic amino acid residues essential for sequence-specific DNA binding activity in vitro, and a carboxy-terminal α-helical domain (helix-loop-helix [HLH]/leucine zipper [LZ]) required for association with the HLH/LZ protein Max (reviewed in reference 12). Current evidence indicates that Myc and Max proteins form heterodimeric complexes that function as sequence-specific transcription factors which likely regulate genes involved in cellular growth and differentiation processes. Additional data suggest that target sequences recognized by the active Myc-Max heterodimeric complex can also be occupied by transactivation-inert Max homodimers that form when intracellular levels of Myc are limiting (6, 23, 26, 29, 32; for reviews, see references 9, 34, and 46). Biological support for this concept is derived from the observation that overexpression of *max* is associated with a dramatic suppression of the transforming activity of Myc in primary cultured cells (29, 32). Thus, the emerging functional data and the biochemical profile of Max support a dual physiological role: not only is Max an obligate DNA-binding partner for Myc, but it also serves to regulate Myc activity in a negative fashion. Furthermore, Max activity may be modulated through mechanisms that include cell cycle-dependent phosphorylation (4).

Members of the Myc family resemble each other in gene and protein structures, in the capacity for malignant transformation, and in the ability to interact with Max (6, 23, 32, 52). In contrast, the three *myc* family genes exhibit marked differences in degree of oncogenic potency, with c-*myc* being most active oncogenically and N- and L-*myc* possessing moderate and weak transforming activities, respectively (3, 10, 32). Furthermore, each gene of the mammalian *myc* family has been shown to be differentially expressed with respect to cell type and developmental stage (for a review, see reference 12). For example, in the midgestational mouse,

* Corresponding author.

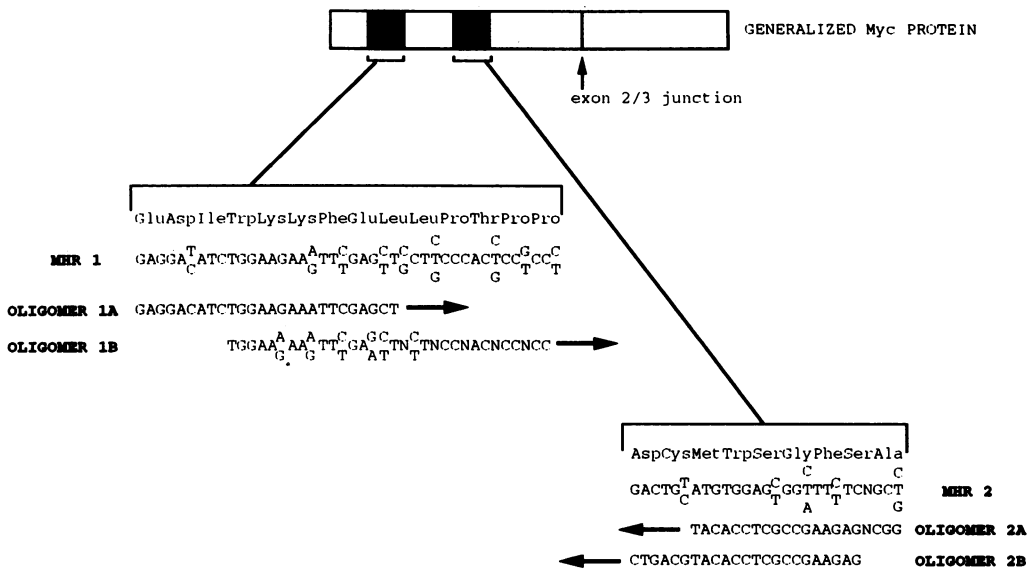

FIG. 1. Nested PCR strategy for the identification of *myc*-specific sequences in the zebra fish genome. Consensus amino acid and nucleic acid sequences for MHR 1 and 2 of previously isolated c-*myc* genes and their relative positions within the second exon-encoded portion of a generalized Myc protein are shown. The nucleic acid sequences of the nested primers used for the amplification of *myc* family homologs from zebra fish genomic DNA are indicated. Oligomers 1A and 1B were the outer and inner primers, respectively, directed to the region designated MHR 1. For MHR 2, the antisense outer primer used was oligomer 2A; the antisense inner primer was oligomer 2B.

c-*myc* gene expression has been observed in a broad range of cell types and has been correlated with active cellular proliferation. In contrast, N- and L-*myc* expression appears restricted to a few cell lineages and correlates more strongly with differentiative processes. Differential patterns of *myc* family gene expression have also been observed in the early stages of both mouse (14) and frog (35, 40, 49, 50) embryogenesis. These differences in oncogenic potency and in temporal and spatial expression patterns, coupled with the observation that each member is conserved as a distinct gene over large evolutionary distances, support the theory that the three *myc* family members serve unique physiological roles.

In this report, we demonstrate that the zebra fish *myc* family, like its mammalian counterpart, consists of three members that exhibit differential patterns of expression and that encode proteins with conserved motifs for DNA binding and protein oligomerization. In addition, we show extensive functional conservation of c-Myc and of the Myc-associated protein Max over an evolutionary distance of approximately 400 million years. The finding that levels of *max* gene expression remain relatively constant while those of the *myc* family vary significantly, as well as the observation that zebra fish *max* (*zmax*) overexpression can suppress mouse c-*myc* (mc-*myc*) transformation activity, supports the current model of the regulation of Myc through alterations in the ratio between Max-Max homodimers and Myc-Max heterodimers. Taken together, the general properties of the *myc* family and *max* appear to be maintained from teleosts to humans, thus enabling one to extrapolate the findings made in the zebra fish with respect to the physiological role of Myc and Max to higher vertebrate systems.

MATERIALS AND METHODS

Fish maintenance and embryo collections. Zebra fish were maintained on a light-dark cycle at 26 to 28.5°C, and eggs were obtained from natural spawnings and staged by cell number during early cleavage. The developmental age of zebra fish embryos was verified visually under a dissecting microscope and is given as hours after fertilization at 28.5°C.

Amplification of *myc* sequences in the zebra fish genome by nested PCR. Primary polymerase chain reaction (PCR) amplifications were performed on zebra fish genomic DNA with 35 cycles in a Perkin-Elmer/Cetus DNA Thermal Cycler, using a cycle of denaturation for 1.0 min at 94°C, annealing for 2.0 min at 40°C, and extension at 72°C for 30 s. Each primary reaction contained 0.5 μg of each outer primer, 2.5 U of *Taq* DNA polymerase (Perkin-Elmer/Cetus), 1.0 μg of zebra fish genomic DNA, 200 μM each deoxynucleoside triphosphate, 4.0 mM $MgCl_2$, and the manufacturer's buffer system in a 100-μl total volume. A 5-μl aliquot of the primary reaction product was used as the template for the secondary amplification of nested PCR. In this secondary reaction, the annealing temperature was raised to 46°C, the $MgCl_2$ concentration was lowered to 2.0 mM, and the inner primers were added. As a control, a 5-μl aliquot of the primary reaction was subjected to a secondary amplification using the original outer primers in place of the inner ones. Outer oligomer 1A and inner oligomer 1B were designed to prime from *myc* homology region (MHR) 1, and outer oligomer 2A and inner oligomer 2B were designed to prime from MHR 2. Their sequences are shown in Fig. 1.

Isolation of zebra fish genomic and cDNA clones and analysis of DNA. For the isolation of c- and N-*myc* homologs, nested-PCR-generated fragments of 201 (zebra fish c-*myc* [zc-*myc*]) and 266 (zebra fish N-*myc* [zN-*myc*]) bp were radiolabeled by the nick translation method and used as probes under normal stringency conditions on an amplified *Sau*3AI-partial, size-selected (15 to 20 kb) genomic library in λEMBL3 (a kind gift of Anders Fjose) and a size-selected (>0.8 kb) oligo(dT)-primed λgt11 cDNA library from 33- to 36-h zebra fish embryos (a kind gift of Kai Zinn). For the isolation of L-*myc* and *max* homologs, these same two libraries were probed under low-stringency conditions (30%

formamide, 37°C) with exon 2 probes derived from *Xenopus* L-*myc*1 (xL-*myc*1) and L-*myc*2 (xL-*myc*2) (a 500-bp *Xho*I-*Pst*I fragment derived from the genomic clone of xL-*myc*1 and a 600-bp *Sty*I fragment derived from the genomic clone of xL-*myc*2 [40]) or a PCR-generated probe containing the coding region of mouse (m*max*). Purification of putative recombinant clones, subcloning, probe preparation by the nick translation method, blotting procedures, and hybridizations were performed as described previously (38). For the single-copy Southern blotting analyses, genomic DNA was derived from individual fish, as the zebra fish is an outbred species. Nucleotide sequencing analysis was performed by the method of Maxam and Gilbert (30), and computer analyses were performed with the Genetics Computer Group sequence analysis software package (13).

Analysis of RNA. Total RNA was isolated by the LiCl-urea method as described previously (2) from various stages of zebra fish embryonic development and from a panel of adult fish tissues. Tissues derived from *Carassius auratus* (also a member of the family Cyprinidae) were used for RNA isolation, since their larger size permitted facile microdissection and sufficient RNA recovery. Twenty micrograms of total RNA was fractionated by electrophoresis through a 0.8% agarose–formaldehyde gel; RNAs were judged to be intact and evenly loaded by ethidium bromide staining and were transferred to nitrocellulose and hybridized as described previously (38). Zebra fish *myc* (z*myc*) family and z*max* probes included: (i) zc-*myc*, a 1.6-kb *Eco*RI fragment from pZc1, (ii) zN-*myc*, a 560-bp *Xmn*I-*Eco*RI fragment derived from the exon 2-homologous region of pZN1, (iii) zebra fish L-*myc* (zL-*myc*), a 1.4-kb *Eco*RI fragment from pZL1 containing exon 2- and 3-homologous sequences, and (iv) z*max*, a 560-bp *Bam*HI-*Xho*I coding region probe and an 1,100-bp *Bam*HI-*Xho*I 3′ untranslated region (UT) probe, both derived from the pZ*max*1 clone. For Northern (RNA) analysis of the transformed rat embryo fibroblast (REF) cell lines, total RNA was isolated as described previously (2) from P19 embryonal carcinoma cells (31), from early-passage nontransformed REFs, and from exponentially growing cultures of mc-*myc*–*ras* or zc-*myc*–*ras*-transformed REF cell lines, and 20 μg of total RNA was used for Northern blotting as described above. RNAs were judged to be intact and evenly loaded by ethidium bromide staining as well as by hybridization to the rat glyceraldehyde-3-phosphate dehydrogenase gene (47). Probes for these Northern analyses included (i) mc-*myc*, a 780-bp *Pst*I-*Xho*I coding domain fragment derived from the c-*myc* cDNA plasmid pMc-*myc*54 (43; a generous gift from Ken Marcu), (ii) zc-*myc*, a 1.6-kb *Eco*RI fragment from pZc1, and (iii) H-*ras*, a 6.4-kb *Bam*HI fragment from pT24-*ras* (15) containing the complete coding region of the mutant human Harvey *ras* gene.

Expression constructs used in REF cooperation assays. For the z*max* expression construct, the 1.8-kb *Eco*RI pZ*max*1-derived fragment, containing complete coding region and extensive 3′ UT, was subcloned into the pVcos7 retroviral vector in the same orientation relative to the Moloney murine leukemia virus long terminal repeat. For the zc-*myc* expression construct, a 2.4-kb *Eco*RI-*Nru*I fragment of the genomic clone (39) containing exon 2 and some exon 3 sequences and a 600-bp *Nru*I-*Eco*RI fragment of pZc1 containing the remainder of exon 3 and a portion of the 3′ UT were subcloned into the pVcos7 retroviral vector in the same orientation relative to the Moloney murine leukemia virus long terminal repeat. The mc-*myc* expression construct was pKO-*myc* (32), in which transcription of exons 2 and 3 of the mc-*myc* gene was driven by a simian virus 40 promoter. The m*max* expression construct was CMV*myn* (kindly provided by Ed Ziff) and consisted of a full-length cDNA encoding the complete m*max* gene driven by the cytomegalovirus promoter/enhancer (33). pT24-*ras* contained the mutant H-*ras* oncogene (Val-12) (15).

Preparation and transfection of REFs. Early-passage cultures of REFs were prepared and cotransfected by the calcium phosphate precipitation method (1) as described previously (32). Transformed foci were analyzed for subcloning efficiency, construct expression, and anchorage independence as described elsewhere (32).

Antibody preparation and Western immunoblot analysis. zc-Myc- and zMax-specific peptides were synthesized, purified by high-pressure liquid chromatography, and mass spectrophotometrically verified by the Macromolecular Analysis Facility at the Albert Einstein College of Medicine. The peptide for zc-Myc was CSEQLKHRLQRLRSSH; the peptide for zMax was CQANYSSSDSSLYTNPK. Peptides were coupled via their N-terminal cysteine residues to maleimide-activated keyhole limpet hemocyanin, using the Imject Activated Immunogen Conjugation Kit (Pierce). Male New Zealand White rabbits were immunized intradermally at multiple sites with peptide-keyhole limpet hemocyanin conjugate in complete Freund's (first boost) or reconstituted Ribi (Ribi Immunochem Research; subsequent boosts) adjuvant. The appearance of anti-zc-Myc or anti-zMax antibodies in the serum was monitored by dot blot analysis against peptide coupled to bovine serum albumin, and both antibodies were affinity purified by chromatography on columns of appropriate peptide linked to agarose beads (Ag/Ab Immobilization Kit 2; Pierce).

For Western blotting analyses, proteins were extracted from the various cell lines by homogenization in 8 M urea or 3% sodium dodecyl sulfate (SDS), separated by SDS-gel electrophoresis (8% gel for zc-Myc and 12% gel for zMax), and electroblotted to nitrocellulose. Blots were blocked for 1 h at 37°C in phosphate-buffered saline containing 10% milk and 0.1% Tween 20, and primary incubations were carried out with a 1:200 dilution of affinity-purified antibody. Donkey anti-rabbit horseradish peroxidase-conjugated whole immunoglobulin G antibody (Amersham) was used at a 1:5,000 dilution as the secondary antibody, and peroxidase activity was detected with enhanced chemiluminescence (Amersham). Controls for nonspecific banding were performed by preincubating the anti-zc-Myc or anti-zMax antibodies (at 1:50 dilutions) with their corresponding synthetic peptides linked to agarose beads (Ag/Ab Immobilization Kit 2; Pierce) for 48 h at 4°C. After centrifugation, a 1:200 dilution of the supernatant was used as the primary antibody in place of the affinity-purified antibody.

Nucleotide sequence accession numbers. The complete nucleic acid sequence of pZc1 was submitted to GenBank under accession number L11710. The complete nucleic acid sequence of pZ*max*1 was submitted to GenBank under accession number L11711.

RESULTS

All three members of the *myc* family and *max* are present in zebra fish. To identify and isolate *myc* family homologs in zebra fish, we devised a PCR cloning strategy that involved two successive stages of PCR amplification with a nested pair of inward-directed primers directed to highly conserved sequences present in the exon 2-encoded portions of previously characterized vertebrate *myc* family genes (Fig. 1; see Materials and Methods for details). Distinct products of

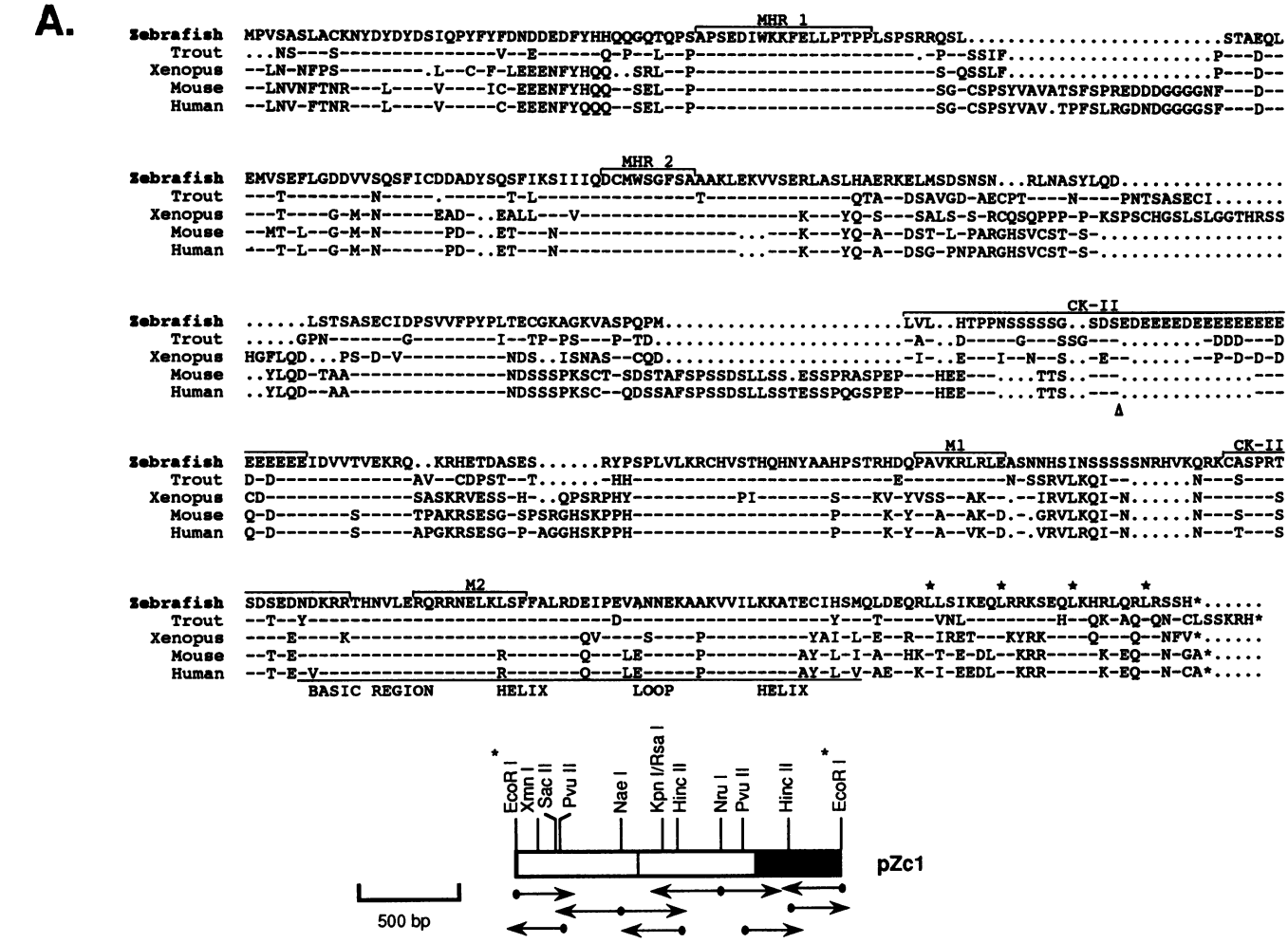

FIG. 2. *zmyc* family members and comparison with vertebrate *myc* homologs. (A) Partial restriction map for pZc1. Open boxes represent regions of the zebra fish clones that possess homology to the coding exon 2 or 3 of other vertebrate c-*myc* genes, and the black box represents the putative 3′ UT. Restriction enzyme sites used in the generation of fragments for sequencing or of probes are indicated. Arrows highlight regions that were sequenced by the method of Maxam and Gilbert (30). Shown above the schematic representation of pZc1 is a comparison of the deduced protein sequence of zc-Myc with the sequences of rainbow trout (48), *Xenopus* (50), mouse (42), and human (16) c-Myc proteins. Amino acid sequences (in single-letter code) were aligned by using the Pileup program of the Genetics Computer Group sequence analysis software package (13) and by visual fit. Position 1 is attributed to the putative initiation codon in exon 2. The sequence of amino acid residues 1 to 14 of the zebra fish protein was derived from nucleic acid sequencing of the genomic clone for zc-*myc* (39), and the remainder was derived from pZc1. Dashes represent identity to the zebra fish residues; dots represent gaps which were introduced in the various c-Myc sequences to maximize homology. The conserved *myc* homology regions (MHR 1 and 2), potential casein kinase II phosphorylation sites (CK-II), nuclear localization motifs (M1 and M2), and basic/HLH regions are indicated. The putative exon 2/3 junction is marked by an

these nested PCRs of 201 and 266 bp were subcloned, subjected to nucleotide sequence analysis, and found to be highly homologous to known c-*myc* and N-*myc* genes, respectively (data not shown). Consequently, these PCR-generated fragments were used for the screening of both an amplified genomic library in the phage vector λEMBL3 constructed from *Sau*3AI partially digested adult zebra fish DNA and an oligo(dT)-primed λgt11 cDNA library from DNA of 33- to 36-h embryos as described in Materials and Methods. Recombinant clones λZc1 and λZN1 were plaque purified on the basis of their homology to nested PCR fragments and to mammalian c-*myc*- and N-*myc*-derived probes. To isolate the zebra fish homologs of L-*myc* and *max* (clones λZL1 and λZmax, respectively), the same genomic and cDNA libraries were probed under low-stringency conditions with radiolabeled xL-*myc* (40) or m*max* genes. Southern blotting analyses demonstrated that each zebra fish *myc* homolog represented a unique single-copy gene (data not shown).

(i) zc-*myc*. Analysis of the sequence of the zc-*myc* cDNA plasmid subclone (pZc1; a partial restriction map is shown in Fig. 2A) and of its genomic clone (39) revealed an ATG-initiated open reading frame capable of encoding a putative zc-Myc protein of 406 amino acids. Amino acid alignment of this protein with other vertebrate c-Myc proteins (Fig. 2A) showed a high degree of conservation; of the amino acids in the deduced zebra fish protein, 77, 65, 63, and 61% were identical in rainbow trout (48), *Xenopus* (50), mouse (42), and human (16) counterparts, respectively. In contrast, alignment of zc-Myc with mouse N- or L-Myc proteins showed identities of only 40%. While the zc-*myc* gene encoded hallmark Myc motifs responsible for nuclear localization, phosphorylation, sequence-specific DNA binding activity, and protein oligomerization, a number of notable differences between zc-Myc and its mammalian homologs were found in regions of potential physiological import. Of particular significance was a sizeable deletion (Fig. 2A; amino acids 70 to 94 of mc-Myc are absent in zc-Myc) within an amino-terminal domain previously shown to be essential for both transforming activity and transactivation potential in the mammalian c-Myc protein (22, 32, 44). Furthermore, a highly acidic domain of unknown function that is located near the exon 2/3 splice junction in other Myc family proteins was strikingly expanded in the zc-Myc protein.

In higher vertebrates, each *myc* family transcript contains a large A+T-rich 3′ UT that is important for the rapid turnover of mature *myc* mRNAs (7, 8, 21). Although the zc-*myc* gene also bears a large A+T-rich 3′ UT, comparisons between zebra fish and mammalian 3′ UTs did not reveal significant nucleotide sequence homologies or obvious conservation of potential hairpin structures (data not shown).

(ii) zN- and zL-*myc*. Regions of the cDNA plasmid subclones pZN1 and pZL1 that bore homology to the second exons of vertebrate *myc* counterparts were localized by both restriction mapping and low-stringency hybridization with mammalian *myc* probes and then subjected to nucleic acid sequencing. The amino acid sequence between the highly conserved MHR 1 and 2 of pZN1 showed 62% identity to the corresponding region of mouse N-Myc (mN-Myc) (Fig. 2B) and only 44 and 49% identity to the corresponding regions of mouse L-Myc (mL-Myc) and mc-Myc, respectively. The high degree of homology between pZN1 and mN-Myc in this focal region indicates that pZN1 represents the zebra fish homolog of N-*myc*. The MHR 1-to-MHR 2 region of pZL1 possessed 64% similarity and 38% identity on the amino acid level to the corresponding region of mL-Myc (Fig. 2C). Notably, this region of pZL1 also exhibited a similar level of homology to vertebrate c-*myc* and N-*myc* genes. However, preliminary sequence analysis of pZL1 in regions known to be divergent among *myc* family genes revealed greater homology to known L-Myc proteins (39), and analysis of expression of this gene showed patterns that were L-*myc*-like in character (see below). Taken together, these results indicate that pZL1 most likely represents the zebra fish L-*myc* homolog.

(iii) *zmax*. Sequence analysis of the cDNA clone p*Zmax*1 showed the presence of an ATG-initiated open reading frame of 155 amino acids that was 89% similar and 86% identical to mammalian Max (Fig. 3). Notably, the basic and leucine zipper regions and the two helices of the HLH region were 100% conserved with human Max (hMax). Amino acid changes were for the most part conservative substitutions that localized to the HLH loop and to the carboxy-terminal region. Despite these carboxy-terminal substitutions, potential casein kinase II phosphorylation sites and a consensus nuclear localization signal appeared intact.

The mammalian *max* gene has been shown to encode several alternatively processed transcripts, one of which contains a 27-nucleotide insertion capable of encoding an additional nine amino acids within the highly acidic amino-terminal region (5, 33). Mammalian *max* mRNAs differing only by this nine-amino-acid segment encode two phosphoproteins of 21 and 22 kDa (6, 52). Characterization of several *zmax* cDNA clones demonstrated that similarly organized transcript forms were present in zebra fish as well (Fig. 3, *Zmax*1 and *Zmax*2). Although the differential activities of these alternative forms remain undetermined, their conservation throughout evolution strongly supports an essential biological role for each form.

***zmyc* family genes and *zmax* exhibit differential patterns of expression during embryogenesis and in adult tissues.** To assess the developmental stage-specific expression of the *zmyc* family and of *zmax*, total RNA was isolated from various embryonic stages between early cleavage and prehatching (18, 19). In Northern blot studies, a zc-*myc*-specific probe detected a low-abundance 2.0-kb transcript in the two-cell through early somite stages (<1.5 through 12 h) that increased markedly in amount during later stages of growth and organ development (Fig. 4A). Levels of a 3.0-kb transcript detected by a zN-*myc*-specific probe increased significantly between 6 and 12 h, a time period characterized by late gastrulation (6 to 9.5 h), early central nervous system

arrowhead, and the conserved leucines of the leucine zipper domain are starred. (B) Amino acid sequence of the open reading frame contained within the nested PCR-amplified region of pZN1 and comparison with the equivalent region in N-Myc (11), as determined by the Gap program of the Genetics Computer Group sequence analysis software package (13). The amino acids of MHR 1 and 2 that are highly conserved are enclosed in boxes. Between the zebra fish and mouse amino acid residues, lines represent identity to the zN-Myc residues, colons represent high homology, and single dots represent weak similarity. Dots in the sequence represent gaps which were introduced in the various N-Myc sequences to maximize homology. (C) The amino acid sequence of the MHR 1-to-MHR 2 region of zL-Myc and the equivalent region of mL-Myc (28). The zL-Myc sequence was derived from nucleic acid sequencing of regions of pZL1 and of its genomic clone (20).

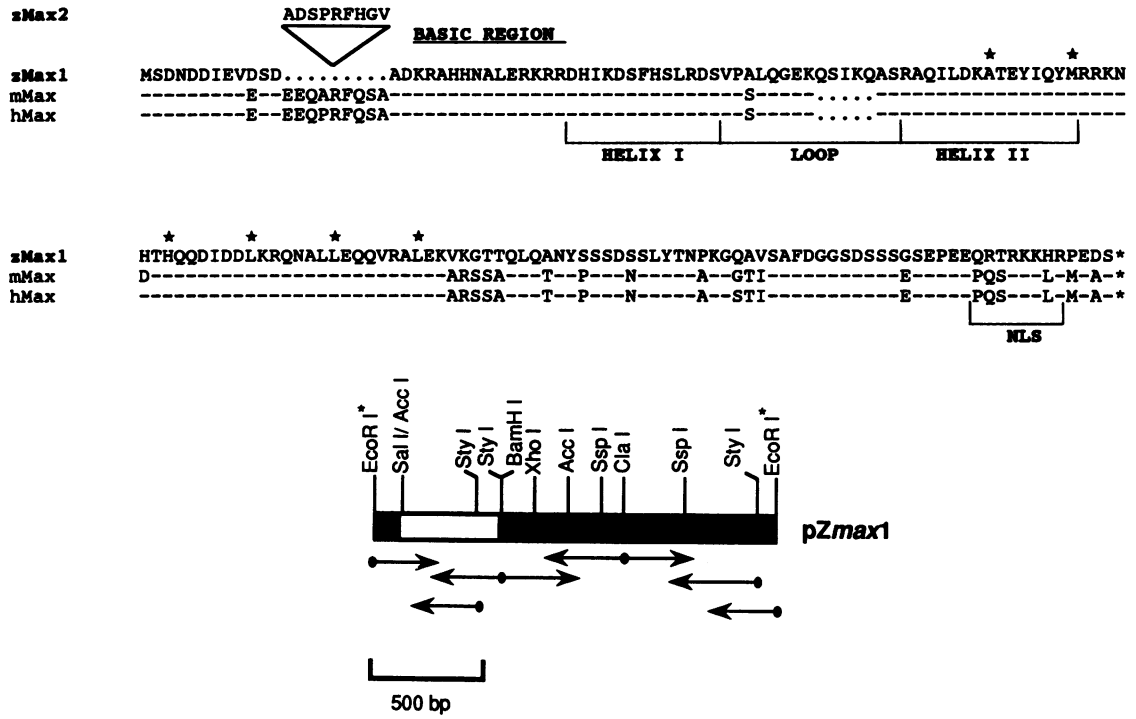

FIG. 3. The *zmax* cDNA clone and comparison of its coding region with those of m*max* and h*max*. A partial restriction map for pZ*max*1 is shown. The open box represents the region possessing sequence homology to and cross-hybridizing with probes derived from the coding region of m*max*, and black boxes represent putative 5′ and 3′ UTs. Arrows indicate portions of the gene sequenced by the method of Maxam and Gilbert (30); *Eco*RI linker sites are those used in cDNA subcloning. Shown above this cDNA clone is a comparison of the putative protein encoded by pZ*max*1 with those encoded by the m*max* (33) and h*max* (5) genes. The nine-amino-acid insertion of a second *max* cDNA clone, pZ*max*2, is also indicated. Amino acid sequences (in single-letter code) were aligned by using the Pileup program of the Genetics Computer Group sequence analysis software package (13). Position 1 is attributed to the putative initiation codon. Dashes represent identity to the zMax residues; dots in the sequence represent gaps which were introduced in the various Max sequences to maximize homology. The basic region, HLH, and nuclear localization signal (NLS) are indicated. Conserved hydrophobic residues of the leucine zipper are starred.

development (8 to 10 h), and early somite formation (10.5 h). Steady-state zN-*myc* mRNA levels continued to increase during stages marked by rapid growth and development of the brain and formation of rudimentary visual and auditory organs and myotomes (12 to 24 h) and remained constant thereafter (Fig. 4B). Expression of the putative zL-*myc* gene differed considerably from that of zc- and zN-*myc*, since its 2.2-kb transcript was most abundant during early rapid cleavage, blastulation, and gastrulation and was found at reduced levels from the time of establishment of the body plan (around 12 h) and thereafter (Fig. 4C). A 1.9-kb *zmax*-specific transcript was detected at relatively constant levels in all stages examined, with a moderate decrease apparent between the 12- and 24-h stages, a time period highlighted by the formation of somites and organ rudiments (Fig. 4D). Because mammalian Max protein has been shown to be extremely stable (6), this observed decrease in *zmax* mRNA levels may not be reflected in a significant reduction in the total zMax pool.

To determine the tissue-specific patterns of *zmyc* family and *zmax* gene expression in fully differentiated adult tissues, total RNA was isolated and was subjected to Northern blotting analysis (Fig. 4). Transcripts of the zc-*myc* and *zmax* genes were observed in a wide variety of tissues, with highest levels present in the kidney, gills, and uterus. Aside from the 1.9-kb transcript, the *zmax* probe also detected a smaller 1.6-kb transcript in the uterus and a larger 2.2-kb transcript in the brain and heart. While the nature of these variant transcripts is unknown, the larger one may represent an alternatively processed form that has been observed in some human cell lines and encodes a truncated Max protein with the potential to enhance Myc transformation activity (29). Of note, however, is the absence of *zmyc* family transcripts in the tissues which contain the larger *max* transcript. The pattern of zN-*myc* and zL-*myc* gene expression in adult tissues differed considerably from that of zc-*myc*, with zN-*myc*-specific transcripts observed at barely detectable levels in most tissues assayed and with zL-*myc*-specific transcripts found in the uterus only.

Cross-species conservation of Max tumor suppression function. It has been proposed that the Max protein serves a dual physiological role (6, 23, 26, 29, 32; for reviews, see references 9, 34, and 46). During periods of active growth and differentiation, high intracellular ratios of Myc to Max support the formation of transactivation-competent Myc-Max heterodimers capable of stimulating transcription of Myc-responsive target genes. During quiescence, Myc levels decrease while Max levels remain constant, thereby promoting the formation of transactivation-incompetent Max-Max homodimers with the capacity to bind Myc-Max target sequences in a repressive manner. Recently, we and others have substantiated this model by demonstrating that overexpression of mammalian Max can induce suppression of Myc-Ras cotransformation activity (29, 32).

To assess whether the highly homologous zMax possessed similar suppressive potential, a *zmax* expression construct

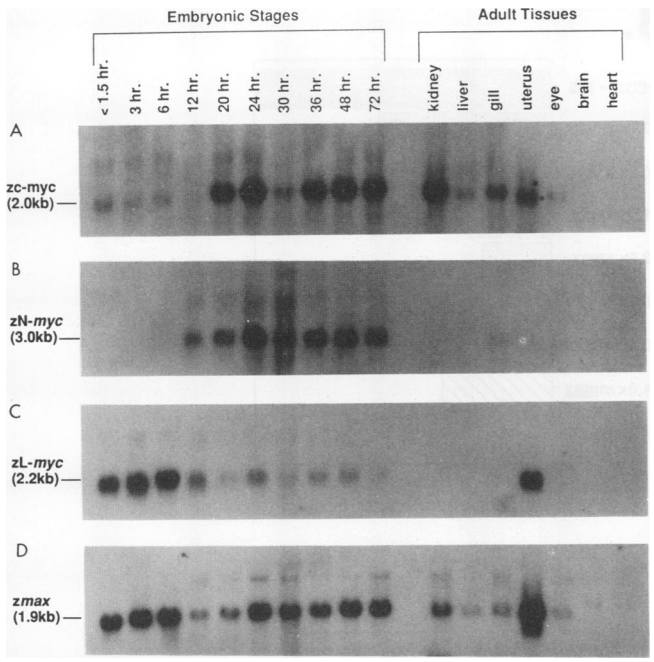

FIG. 4. Northern blot analysis of the distribution of zc-, zN-, and zL-*myc* and *zmax* transcripts during zebra fish embryogenesis and in adult fish tissues. Total RNAs derived from the embryonic stages and tissues specified were assayed for hybridization to ^{32}P-labeled zc-*myc* (A), zN-*myc* (B), zL-*myc* (C), and *zmax* (D) probes. The same Northern blot was successively hybridized and stripped; complete dehybridization was verified by autoradiography. Hours after fertilization at 28.5°C correspond roughly to the times of the following developmental events: <1.5 h, early cleavage; 3 h, mid-blastula; 6 h, gastrula (50% epiboly); 12 h, early somite formation; 20 h, auditory placode development; 24 h, optic cup and otolith formation; 30 h, heartbeat and circulation initiation; 36 h, retinal pigmentation; 48 h, body pigmentation (melanophores); and 72 h, body pigmentation (xanthophores) and prehatching (18, 19).

was cotransfected with mc-*myc* and activated H-*ras* expression constructs into early-passage REFs (27). The *zmax* expression construct consisted of a 1.8-kb *Eco*RI pZ*max*1-derived fragment, containing the complete coding domain and 3′ UT, subcloned into the pVcos7 retroviral vector in the same transcriptional orientation relative to the Moloney murine leukemia virus long terminal repeat. As shown in Fig. 5A, the addition of a 2.5-fold molar excess of the *zmax* expression construct to mc-*myc*–*ras* cotransfections was associated with a striking reduction in focus formation compared with the number of foci generated by mc-*myc*–*ras* alone (Fig. 5A, experiment 1). Notably, the degree of this reduction was similar to that caused by the addition of an equivalent amount of an m*max* expression construct to mc-*myc*–*ras* cotransfections (Fig. 5A, experiment 1). Consistent with the proposed model, the relative molar ratio of transfected *zmax* to mc-*myc* proved to be an important parameter, as an increase in the amount of added *zmax* was found to correlate with a progressive reduction in the number of foci generated (Fig. 5A, experiment 2; Fig. 5B).

zc-*myc* can function as an oncogene in mammalian cells. To determine the degree of cross-species functional relatedness of Myc oncoproteins, a zc-*myc* expression construct was tested for its ability to cooperate with activated H-*ras* to effect the malignant transformation of early-passage REFs. In several transfections, the zc-*myc* construct generated a slightly lower number of foci in the monolayer compared with the control mc-*myc* expression construct (Fig. 5C). In addition, by several criteria, the oncogenic potency of zc-*myc* appeared somewhat diminished in comparison with that of mc-*myc*. Morphologically, foci generated by the zebra fish expression construct exhibited a more mildly transformed phenotype (data not shown). With regard to subcloning efficiency, that of zc-*myc*–*ras* generated foci was only 33%, compared with the 67% observed with mc-*myc*–*ras*-generated foci. When assayed for anchorage-independent growth, 8 of 14 mc-*myc*–*ras*-transformed lines (57%), but only 3 of 14 zc-*myc*–*ras*-transformed lines (21%) were capable of colony formation in soft agar.

Several permanently established zc-*myc*–*ras*-transformed cell lines were analyzed for steady-state mRNA expression by Northern blotting and were shown to express high levels of the 2.0-kb transcript encoded by the transfected zc-*myc* gene (Fig. 6A, zebra fish c-*myc* panel, lanes 5 to 8). These levels were comparable to those generated by the transfected mc-*myc* gene in mc-*myc*–*ras*-transformed lines (Fig. 6A, mouse c-*myc* panel, lanes 1 to 4) and were highly increased relative to the level of c-*myc* gene expression found in the P19 mouse embryonal carcinoma cell line, a cell line that serves as a control for the level of *myc* family gene expression typically observed in developing mouse tissues (Fig. 6A, mouse c-*myc* panel, lane P19). In addition, all transformed cell lines were found to express high steady-state mRNA levels of the introduced H-*ras* gene (Fig. 6A; H-*ras* panel, lanes 1 to 8).

Analysis of expression of the introduced zc-*myc* gene on the protein level by Western blotting showed the presence of a major 50-kDa protein and a minor 57-kDa protein in zc-*myc*–*ras*-transformed cell lines (Fig. 6B, lane 1). While the precise nature of these two forms remains to be determined, they both appear to be zc-Myc specific. Notably, these bands were absent from mc-*myc*–*ras*-transformed and early-passage nontransformed REF cell lines (Fig. 6B, lanes 2 and 3, respectively) and were undetectable when the anti-zc-Myc antibody was preincubated with the immunogenic zc-Myc peptide before use (Fig. 6B, lanes 4 to 6). Finally, when similar analyses were applied to study protein expression of transfected genes in *zmax*–mc-*myc*–*ras*-transformed cell lines, a distinct 24-kDa protein band was observed (Fig. 6B, lane 7) and found to be zMax specific (Fig. 6B, lanes 8 to 12).

DISCUSSION

In this study, we have compared structural and functional features of the *zmyc* family and *zmax* genes with those of higher vertebrate counterparts. The conservation of structures shown previously to be essential for transactivation potential, nuclear localization, protein-protein interaction (HLH/LZ region) and sequence-specific DNA binding activity (basic region) suggests that the putative function of the Myc-Max complex as a regulator of gene expression has been maintained throughout vertebrate evolution. Furthermore, the complete conservation of DNA binding and dimerization sequences in the Max protein from fish to humans may reflect a process in which intense structural constraints are imposed by a requirement for interaction with many different Max-associated proteins, namely, c-Myc, N-Myc, and L-Myc (6, 23, 32, 52) and newly described negative regulators of Myc function, Mad (2a) and Mxi1 (52a).

On the functional level, *zmax* appeared to be equivalent to mammalian *max*, as it too could suppress the transformation

A.

TRANSFECTED DNA		Exp 1 TOTAL # OF FOCI	Exp 2 TOTAL # OF FOCI
mc-myc + ras		273	463
+ zmax	0.1x	-	275
	0.5x	-	220
	1.0x	-	111
	2.5x	83	107
+ mmax	0.1x	-	276
	0.5x	-	207
	1.0x	-	169
	2.5x	59	81
pVcos7 + ras		3	-

B.

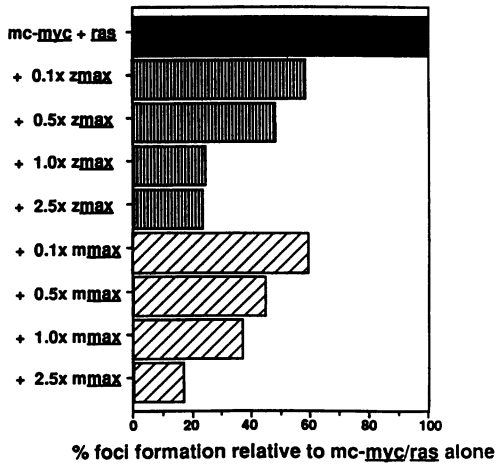

C.

TRANSFECTED DNA	Exp. 1	Exp. 2	Exp. 3		
	foci count	foci count	foci count	Subcloning efficiency	Anchorage independence
mc-myc + ras	142/6	177/6	81/12	16/24 (67%)	8/14 (57%)
zc-myc + ras	88/6	107/6	80/12	8/24 (33%)	3/14 (21%)
pVcos7 + ras	2/6	-	-	-	-

FIG. 5. Conservation of *max* tumor suppressor function and c-*myc* oncogenic activity in the REF assay. (A) The total number of foci on nine plates derived from three transfected plates was counted 9 to 11 days after transfection. Each plate was transfected with 2 μg of mc-*myc*, 2 μg of activated *ras*, 30 μg of mouse liver carrier DNA, and either 0.0 μg (mc-*myc* + *ras* row), 0.2 μg (0.1× rows), 1 μg (0.5× rows), 2 μg (1.0× rows), or 5 μg (2.5× rows) of the appropriate *max* expression construct as indicated in the transfected DNA column. As a negative control, 2 μg of the pVcos7 vector without insert was cotransformed with 2 μg of activated *ras* and 30 μg of carrier DNA. Dashes represent experimental points that were not determined. (B) Histogram of data in transfection 2 in panel A. Percent focus formation was derived by expressing the total number of foci counted in the various *max* transfections as a percentage of the total number of foci counted in the mc-*myc*–*ras*-only transfection. (C) Each plate was transfected with 2 μg of the appropriate c-*myc* plasmid, 2 μg of activated *ras*, and 30 μg of carrier DNA. As a negative control, 2 μg of the pVcos7 vector without insert was cotransformed with 2 μg of activated *ras* and 30 μg of carrier DNA. Foci count is expressed as the total number of foci over the total number of plates, subcloning efficiency is expressed as the total number of established cell lines over the total number of cell lines tested, and anchorage independence is expressed as the number of anchorage-independent lines over the total number of lines tested. Dashes represent experimental points that were not determined.

activity of mc-*myc* in the REF cooperation assay. The zc-*myc* gene, while capable of cooperating with an activated H-*ras* gene to effect the malignant transformation of primary mammalian cells, exhibited reduced oncogenic potency compared with its mammalian counterpart. Although the basis for this diminished oncogenicity remains to be determined, several possibilities are (i) structural differences between zebra fish and mouse c-Myc that localize to the amino terminus, specifically in regions that have been shown previously to be involved in both transactivation and transformation (22, 32, 44), (ii) negative regulatory elements in the region upstream of the zc-*myc* initiator codon, (iii) cross-species incompatibility for associated cellular proteins, and/or (iv) reduced stability of the zc-Myc protein, perhaps resulting from its expanded acidic domain. Notwithstanding these minor differences in oncogenic potency, the overall findings of the transformation experiments described in this study suggest strong conservation of c-Myc and Max function throughout vertebrate evolution, thus enabling one to exploit the zebra fish system for its unique experimental advantages and then apply deduced models of the physiological role of Myc and Max to higher organisms as well.

The markedly different patterns of expression of the three *myc* family genes during zebra fish embryonic development support the theory that they each serve essential and distinct physiological roles therein. During the earliest stages of embryogenesis, i.e., those typified by rapid growth of immature cell types, levels of zL-*myc* maternally derived transcripts were found to be extremely high, whereas those of zc- and zN-*myc* were barely detectable or absent altogether. Cellular commitment and early differentiative processes that accompany gastrulation were associated with a substantial decrease in zL-*myc* transcript levels, presumably a result of degradation of zL-*myc* maternal mRNAs. This pattern supports a role for zL-*myc* as either an activator in early proliferation of immature cell types or an inhibitor of early cellular differentiation or both.

Myc family gene expression during zebra fish embryogenesis contrasts sharply with that observed during pregastrulation stages of frog and mouse development, in which

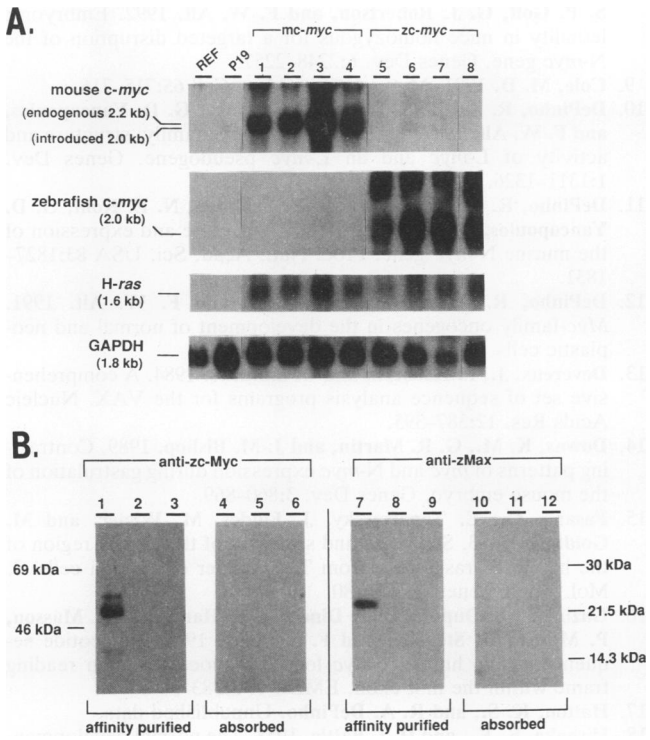

FIG. 6. Expression of introduced zebra fish genes in stably transformed REF cell lines. (A) Twenty micrograms of total RNA derived from P19 cells, from early-passage nontransformed REFs, and from mc-*myc*-transformed (lanes 1 to 4) or zc-*myc*-transformed (lanes 5 to 8) cell lines was subjected to Northern blotting analysis using radiolabeled fragments specific to probes indicated at the left. Blots were hybridized with radiolabeled probes of similar specific activities, and exposures were for similar lengths of time. (B) In lanes 1 to 6, 15 μg of total protein extracted from zc-*myc*-transformed (lanes 1 and 4) or mc-*myc*-transformed (lanes 2 and 5) cell lines or from early-passage nontransformed REFs (lanes 3 and 6) was fractionated on an SDS–8% polyacrylamide gel. In lanes 7 to 12, 15 μg of total protein extracted from *zmax*–mc-*myc*-transformed (lanes 7 and 10) or m*max*–mc-*myc*-transformed (lanes 8 and 11) cell lines or from early-passage nontransformed REFs (lanes 9 and 12) was fractionated on an SDS–12% polyacrylamide gel. Primary antibodies used were affinity-purified anti-zc-Myc (lanes 1 to 3), preabsorbed anti-zc-Myc (lanes 4 to 6), affinity-purified anti-zMax (lanes 7 to 9), and preabsorbed anti-zMax (lanes 10 to 12). Locations of Rainbow protein molecular weight markers (Amersham) are indicated on the left for the 8% gel and on the right for the 12% gel.

transcripts of all three *myc* family genes were readily detected (17, 40). If Myc family function is indeed required for cellular growth during embryogenesis, then the consistent presence of L-*myc* expression in early vertebrate development would suggest that L-Myc alone could assume this growth-related role. This possibility is compatible with findings obtained in the mouse system, wherein animals bearing homozygous null mutations of N- (8a, 41a) or c-*myc* (7a) grow and survive well beyond early gestational stages. Furthermore, RNA in situ hybridization performed upon early-stage mouse embryos has shown a poor correlation between c-*myc* gene expression and cellular proliferation (14); perhaps L-Myc and not c-Myc is involved in the control of the rapid cell divisions that typify early vertebrate embryogenesis. As an alternative possibility, if all three members of the *myc* family function in an equivalent manner at this early developmental stage, then significant species variability in the pattern of expression would be tolerated if at least one member were expressed and could readily compensate for the absence of other members. This compensation may operate only during early embryogenesis and may be replaced by unique roles for each *myc* family member as cell lineages become increasingly differentiated. Production of a homozygous null mutation of L-*myc* will ultimately allow for the resolution of these two possibilities.

Although zygotic transcription in the zebra fish begins at the midblastula stage (25), levels of zN-*myc* transcripts do not accumulate significantly until after gastrulation, during a developmental period characterized by formation of a number of early embryonic structures. In the frog and mouse, early embryonic distribution of N-*myc* mRNA has been observed in the central nervous system, the neural crest, and the somites (14, 49). Since the increase in expression of zN-*myc* between 6 and 18 h postfertilization in the zebra fish embryo coincides with the establishment of similar structures, the cross-species conservation of temporal expression is consistent with a role for N-*myc* in events such as neurogenesis. The observation that high levels of zN-*myc* embryonic expression are significantly downregulated in terminally differentiated adult tissues likely indicates that the function of N-*myc* is restricted solely to the growth and development of the zebra fish embryo.

For zc-*myc*, high-level gene expression was apparent at later stages of development, particularly during periods of active cellular proliferation in developing organ systems. Similarly, in the midgestational mouse embryo, abundant expression of the c-*myc* gene was found to be broadly distributed and to correlate well with active cellular proliferation in developing tissues (for a review, see reference 12). Levels of zc-*myc* transcripts were also high in several adult tissues, including kidney, gills, and liver; the coordinate expression of the *zmax* gene in these same tissues suggests that the zc-Myc–Max complex may serve an active physiological role therein. In mammalian terminally differentiated tissues, *myc* family gene expression is low or absent altogether (53). In contrast, continued high-level expression of c-*myc* in various adult tissues of fish and frogs (40) is consistent with a distinctive role for c-Myc in lower vertebrate-specific processes such as regeneration. Furthermore, this high level of c-*myc* gene expression in adult tissues may correlate with the high incidence of neoplasia observed in fish (41). The isolation of c-*myc* and other *myc*-related sequences in zebra fish will now permit investigation into their role in tumorigenesis in teleosts.

The significant alterations in steady-state *myc* family gene expression during zebra fish embryogenesis were paralleled by nearly constant levels of *zmax* gene expression. Similarly, nearly constitutive levels of *max* steady-state mRNA have been observed in mammalian cells regardless of their proliferative or differentiative states (6, 51). Recent data have suggested that the relative intracellular levels of Myc and Max serve to influence the transcriptional activation of Myc-responsive gene targets (6, 23, 26, 29, 32; for reviews, see references 9, 34, and 46). This process appears to be mediated through a dynamic interchange between the formation of active Myc-Max heterodimers and transactivation-incompetent Max-Max homodimers. The patterns of developmental expression described in this study are consistent with a model in which Myc-related developmental activities are controlled principally through the regulation of *myc* family, as opposed to *max*, gene expression.

Isolation of the entire *myc* family and *max* in an accessible

developmental genetic system affords the opportunity to determine the role and regulation of each Myc family member in normal vertebrate embryogenesis, particularly in light of the fact that Myc and Max function appears conserved throughout evolution. With the capacity for microinjection of functional synthetic mRNAs into developing embryos, the zebra fish system would permit an examination of the developmental consequences of inappropriate early-stage zN- or zc-*myc* expression. Furthermore, by introducing chimeric *myc* transcripts in which domains that encode transactivation potential or sequence-specific DNA binding activity have been exchanged between species or between family members, one can readily establish structure-function relationships of physiological significance and assign differential activities to the various *myc* family members. Finally, the microinjection of dominant negative forms of Myc family proteins or an excess of Max would ascertain the requirement for Myc in early vertebrate growth and development and serve to test the current hypothesis of Myc and Max regulation.

ACKNOWLEDGMENTS

We thank Salome Waelsch, Ken Krauter, Art Skoultchi, and Fred Alt for critical reading of the manuscript. We are indebted to Raanan Agus for computer assistance and Joseph DePinho for graphic artwork.

N.S.-A. is supported by NIH training grant T32 GM07128, and R.T. is supported by NIH training grant CA09173-14. J.H. is supported by Cancer Center Core NIH grant 2P30CA13330-20. R.A.D. is supported by NIH grants RO1 EY09300-01 and RO1 HD28317-01. R.A.D. is a recipient of the McDonnell Foundation Scholar Award, an American Heart Association Established Investigatorship Award, and a Cancer Research Institute Investigator Award. R.A.D. was aided by Basil O'Connor Starter Scholar Research Award 5-724 through funds received from the Lifespring Foundation to the March of Dimes Defects Foundation.

REFERENCES

1. **Andersson, P., M. P. Goldfarb, and R. A. Weinberg.** 1979. A defined subgenic fragment of *in vitro* synthesized Moloney sarcoma virus DNA can induce cell transformation upon transfection. Cell **16**:63–75.
2. **Auffray, C., and F. Rougeon.** 1980. Purification of mouse immunoglobulin heavy chain messenger RNAs from total myeloma tumor RNA. Eur. J. Biochem. **107**:303–314.

2a. **Ayer, D. E., L. Kretzner, and R. N. Eisenman.** 1993. Mad: a heterodimeric partner for Max that antagonizes Myc transcriptional activity. Cell **72**:211–222.

3. **Barrett, J., M. J. Birrer, G. J. Kato, H. Dosaka-Akita, and C. V. Dang.** 1992. Activation domains of L-Myc and c-Myc determine their transforming potencies in rat embryo cells. Mol. Cell. Biol. **12**:3130–3137.
4. **Berberich, S. J., and M. D. Cole.** 1992. Casein kinase II inhibits the DNA-binding activity of Max homodimers but not Myc/Max heterodimers. Genes Dev. **6**:166–176.
5. **Blackwood, E. M., and R. N. Eisenman.** 1991. Max: a helix-loop-helix zipper protein that forms a sequence-specific DNA binding complex with Myc. Science **251**:1211–1217.
6. **Blackwood, E. M., B. Luscher, and R. N. Eisenman.** 1992. Myc and Max associate in vivo. Genes Dev. **6**:71–80.
7. **Bonnieu, A., M. Piechaczyk, L. Marty, M. Cuny, J.-M. Blanchard, P. Fort, and P. Jeanteur.** 1988. Sequence determinants of c-*myc* mRNA turn-over: influence of 3′ and 5′ non-coding regions. Oncogene Res. **3**:155–166.

7a. **Bradley, A.** Personal communication.

8. **Brewer, G., and J. Ross.** 1988. Poly(A) shortening and degradation of the 3′ AU-rich sequences of human c-*myc* mRNA in a cell-free system. Mol. Cell. Biol. **8**:1697–1708.

8a. **Charron, J., B. A. Malynn, P. Fisher, V. Stewart, L. Jeanotte, S. P. Goff, G. J. Robertson, and F. W. Alt.** 1992. Embryonic lethality in mice homozygous for a targeted disruption of the N-*myc* gene. Genes Dev. **6**:2248–2257.

9. **Cole, M. D.** 1991. Myc meets its Max. Cell **65**:715–716.
10. **DePinho, R. A., K. S. Hatton, A. Tesfaye, G. D. Yancopoulos, and F. W. Alt.** 1987. The human *myc* gene family: structure and activity of L-*myc* and an L-*myc* pseudogene. Genes Dev. **1**:1311–1326.
11. **DePinho, R. A., E. Legouy, L. B. Feldman, N. E. Kohl, G. D. Yancopoulos, and F. W. Alt.** 1986. Structure and expression of the murine N-*myc* gene. Proc. Natl. Acad. Sci. USA **83**:1827–1831.
12. **DePinho, R. A., N. Schreiber-Agus, and F. W. Alt.** 1991. *Myc*-family oncogenes in the development of normal and neoplastic cells. Adv. Cancer Res. **57**:1–46.
13. **Devereux, J., P. Haeberli, and O. Smithies.** 1984. A comprehensive set of sequence analysis programs for the VAX. Nucleic Acids Res. **12**:387–395.
14. **Downs, K. M., G. R. Martin, and J. M. Bishop.** 1989. Contrasting patterns of *myc* and N-*myc* expression during gastrulation of the mouse embryo. Genes Dev. **3**:860–869.
15. **Fasano, O., E. Taparowsky, J. Fiddes, M. Wigler, and M. Goldfarb.** 1983. Sequence and structure of the coding region of the human H-ras-1 gene from T24 bladder carcinoma cells. J. Mol. Appl. Genet. **2**:173–180.
16. **Gazin, C., S. Dupont, D. de Dinechin, A. Hampe, J. M. Masson, P. Martin, D. Stehelin, and F. Gailbert.** 1984. Nucleotide sequence of the human c-*myc* locus: provocative open reading frame within the first exon. EMBO J. **3**:383–387.
17. **Hatton, K. S., and R. A. DePinho.** Unpublished data.
18. **Hisaoka, K. K., and H. I. Battle.** 1958. The normal developmental stages of the zebrafish, Brachydanio Rerio (Hamilton-Buchanan). J. Morphol. **102**:311–327.
19. **Hisaoka, K. K., and C. Firlit.** 1960. Further studies on the embryonic development of the zebrafish, Brachydanio Rerio (Hamilton-Buchanan). J. Morphol. **107**:205–225.
20. **Horner, J., and R. A. DePinho.** Unpublished data.
21. **Jones, T. R., and M. D. Cole.** 1987. Rapid cytoplasmic turnover of c-*myc* mRNA: requirement of the 3′ untranslated sequences. Mol. Cell. Biol. **7**:4513–4521.
22. **Kato, G. J., J. Barret, M. Villa-Garcia, and C. V. Dang.** 1990. An amino-terminal c-Myc domain required for neoplastic transformation activates transcription. Mol. Cell. Biol. **10**:5914–5920.
23. **Kato, G. J., W. M. F. Lee, L. Chen, and C. V. Dang.** 1992. Max: functional domains and interaction with c-Myc. Genes Dev. **6**:81–92.
24. **Kenyon, C.** 1988. The nematode *Caenorhabditis elegans*. Science **240**:1448–1453.
25. **Kimmel, C.** 1989. Genetics and early development of zebrafish. Trends Genet. **5**:283–288.
26. **Kretzner, L., E. M. Blackwood, and R. N. Eisenman.** 1992. Myc and Max proteins possess distinct transcriptional activities. Nature (London) **359**:426–429.
27. **Land, H., L. F. Parada, and R. A. Weinberg.** 1983. Tumorigenic conversion of primary embryo fibroblasts requires at least two cooperating oncogenes. Nature (London) **304**:596–602.
28. **Legouy, E., R. A. DePinho, K. Zimmerman, R. Collum, G. Yancopoulos, L. Mitsock, R. Kriz and F. W. Alt.** 1987. Structure and expression of the murine L-*myc* gene. EMBO J. **6**:3359–3366.
29. **Makela, T. P., P. J. Koskinen, I. Vastrik, and K. Alitalo.** 1992. Alternative forms of Max as enhancers or suppressors of Myc-Ras cotransformation. Science **256**:373–376.
30. **Maxam, A., and W. Gilbert.** 1980. Sequencing end-labeled DNA with base-specific chemical cleavages. Methods Enzymol. **65**: 499–560.
31. **McBurney, M. W., E. M. V. Jones-Villeneuve, M. R. S. Edwards, and P. T. Andersen.** 1982. Control of muscle and neuronal differentiation in a cultured embryonal carcinoma cell line. Nature (London) **299**:165–167.
32. **Mukherjee, B., S. D. Morgenbesser, and R. A. DePinho.** 1992. Myc-family oncoproteins function through a common pathway to transform normal cells in culture: cross interference by Max

and trans-acting dominant mutants. Genes Dev. **6**:1480–1492.
33. **Prendergast, G. C., D. Lawe, and E. B. Ziff.** 1991. Association of Myn, the murine homolog of Max, with c-Myc stimulates methylation-sensitive DNA binding and Ras cotransformation. Cell **65**:395–407.
34. **Prendergast, G. C., and E. B. Ziff.** 1992. A new bind for Myc. Trends Genet. **8**:91–96.
35. **Principaud, G., and G. Spohr.** 1991. *Xenopus laevis* c-*myc* I and II genes: molecular structure and developmental expression. Nucleic Acids Res. **19**:3081–3088.
36. **Rossant, J., and N. Hopkins.** 1992. Of fin and fur: mutational analysis of vertebrate embryonic development. Genes Dev. **6**:1–13.
37. **Rubin, G. M.** 1988. *Drosophila melanogaster* as an experimental organism. Science **240**:1453–1459.
38. **Sambrook, J., E. F. Fritsch, and T. Maniatis.** 1989. Molecular cloning: a laboratory manual, 2nd ed. Cold Spring Harbor Laboratory Press, Cold Spring Harbor, N.Y.
39. **Schreiber-Agus, N., and R. A. DePinho.** Unpublished data.
40. **Schreiber-Agus, N., R. Torres, J. Horner, A. Lau, M. Jamrich, and R. A. DePinho.** 1993. Comparative analysis of the expression and oncogenic activities of *Xenopus* c-, N-, and L-*myc* homologs. Mol. Cell. Biol. **13**:2456–2468.
41. **Sindermann, C. J.** 1979. Pollution-associated diseases and abnormalities of fish and shellfish. Fish. Bull. **76**:717–749.
41a. **Stanton, B. R., A. S. Perkins, L. Tessarollo, D. A. Sassoon, and L. F. Parada.** 1992. Loss of N-*myc* function results in embryonic lethality and failure of epithelial component of the embryo to develop. Genes Dev. **6**:2235–2247.
42. **Stanton, L. W., P. D. Fahrlander, P. M. Tesser, and K. B. Marcu.** 1984. Nucleotide sequence comparison of normal and translocated murine c-*myc* genes. Nature (London) **310**:423–425.
43. **Stanton, L. W., R. Watt, and K. B. Marcu.** 1983. Translocation, breakage and truncated transcripts of the c-*myc* oncogene in murine plasmacytomas. Nature (London) **303**:401–406.
44. **Stone, J., T. deLange, G. Ramsay, F. Jakobovits, J. M. Bishop, H. Varmus, and W. Lee.** 1987. Definition of regions in human c-*myc* that are involved in transformation and nuclear localization. Mol. Cell. Biol. **7**:1697–1709.
45. **Streisinger, G., C. Walker, N. Dower, D. Knauber, and F. Singer.** 1981. Production of clones of homozygous diploid zebra fish (*Brachydanio rerio*). Nature (London) **291**:293–296.
46. **Torres, R., N. Schreiber-Agus, S. D. Morgenbesser, and R. A. DePinho.** 1992. Myc and Max: a putative transcriptional complex in search of a cellular target. Curr. Opin. Cell Biol. **4**:468–474.
47. **Tso, J. Y., X.-H. Sun, T.-H. Kao, K. S. Reece, and R. Wu.** 1985. Isolation and characterization of rat and human glyceraldehyde-3-phosphate dehydrogenase cDNAs genomic complexity and molecular evolution of the gene. Nucleic Acids Res. **13**:2485–2502.
48. **Van Beneden, R. J., D. K. Watson, T. T. Chen, J. A. Lautenberger, and T. S. Papas.** 1986. Cellular *myc* (c-*myc*) in fish (rainbow trout): its relationship to other vertebrate *myc* genes and to the transforming genes of the MC29 family of viruses. Proc. Natl. Acad. Sci. USA **83**:3698–3702.
49. **Vize, P. D., A. Vaughan, and P. Krieg.** 1990. Expression of the N-*myc* protooncogene during the early development of *Xenopus laevis*. Development **110**:885–896.
50. **Vriz, S., M. Taylor, and M. Mechali.** 1989. Differential expression of two *Xenopus* c-*myc* protooncogenes during development. EMBO J. **8**:4091–4097.
51. **Wagner, A. J., M. M. Le Beau, M. O. Diaz, and N. Hay.** 1992. Expression, regulation, and chromosomal localization of the Max gene. Proc. Natl. Acad. Sci. USA **89**:3111–3115.
52. **Wenzel, A., C. Cziepluch, U. Hamann, J. Schurmann, and M. Schwab.** 1991. The N-Myc oncoprotein is associated *in vivo* with the phosphoprotein Max (p20/22) in human neuroblastoma cells. EMBO J. **10**:3703–3712.
52a. **Zervos, A. S., J. Gyuris, and R. Brent.** 1993. Mxi1, a protein that specifically interacts with Max to bind Myc-Max recognition sites. Cell **72**:223–232.
53. **Zimmerman, K. A., G. D. Yancopoulos, R. G. Collum, R. K. Smith, N. E. Kohl, K. A. Denis, M. M. Nau, O. N. Witte, D. Toran-Allerand, C. E. Gee, J. D. Minna, and F. W. Alt.** 1986. Differential expression of *myc* family genes during murine development. Nature (London) **319**:780–783.